

Original Study

Open Access

H. Ayeche*, Z. Zitouni, A. Limam, A. Bouafia

Parametric study of the earth dam's behaviour subjected to earthquake

<https://doi.org/10.2478/sgem-2022-0017>

received January 14, 2022; accepted July 3, 2022.

Abstract: Static stability of an earth dam can be established by estimating the static safety factor equal to the ratio of the shear strength to the shear stress along a critical sliding area. In contrast, it is more complicated to evaluate the dynamic stability during an earthquake. The water filling the interstices of the earth dams cannot drain during the short duration of an earthquake. An excess pore water pressure ΔU develops, and its role is predominant in the destabilisation of the dam. The pore water increase causes a decrease in the soil shear strength. It is, therefore, crucial to evaluate and take into consideration ΔU in the dam dynamic stability analysis. This research is a contribution to reach this objective. A parametric study was conducted by varying the physical and mechanical soil characteristics constituting the dam, as well as its geometrical values, in order to evaluate their effects on the dynamic safety factor. The dynamic safety factor is calculated using the pseudo-static method, taking into account the excess pore water pressure that develops during cyclic loading into the granular soil of the earth dam upstream face. The results of the parametrical analytical study were also compared to the results of numerical simulations of the dam seismic stability through pseudo-static method. The numerical simulations were done with three different software: PLAXIS and ABAQUS (based on the finite element method) and GEOSTAB (deals with the problem at the limit equilibrium using the simplified Bishop method). At the end, on one hand, we were able to describe how and at what level of the dam upstream face the sliding occurs, and on the other hand, we were able to underline the adequate combination between the dam geometric parameters and the mechanical soil characteristics which may ensure seismic stability.

Keywords: Earth dam; earthquake; slope stability; block method; Sarma method.

1 Introduction

Dams can ensure several functions such as agricultural irrigation, water supply, hydroelectric power generation and flood cutter. Concrete dams and embankment dams represent about 85% of the dams all over the world. Embankment dams can be classified into two main categories: earth-fill dams and rock-fill dams. Earth-fills dam can be classified into homogeneous material dams and core/zoned dams. Homogeneous dam is the one that uses the same materials throughout, and core/zoned dam is a type of earthen dam where a compacted central clay core is supported on the upstream and downstream sides by compacted materials (Fig. 1). In the latest case, the core material is different from the shell materials, in particular, with less permeability. The core may be designed to be placed in the centre of the dam or elsewhere and may be vertical or tilted as needed according to the upstream and downstream slopes of the dam.

Earthen dam structures are very important to the development of human society since the civilisation began. Despite significant development in geotechnical engineering, it was observed that earthquakes continue to cause failure of many dams and, in certain cases, they result in catastrophic destruction (Tani, 1996). A comprehensive summary of the known earthquake damages to 58 earth dams was prepared by Ambraseys (1960) and was revised by Basudhar et al. (2010), where important dams' failures were reported briefly. The 2011 off the Pacific Coast of Tohoku Earthquake damaged about 750 dams among the 3730 small earth dams in Fukushima Prefecture; the observed failure modes included slide failure and the lateral deformation of embankments (Hori et al., 2012; Mohri et al., 2014). The seismic performance of earth-fill dams with reservoirs of water has also been examined by some researchers, mainly with dynamic centrifuge tests (Kim et al., 2011) and large-scale shaking table test (Yuan et al., 2014). Until now, the research works

*Corresponding author: H. Ayeche, University of Blida 1, Algeria, E-mail: hafida_ayeche@yahoo.fr

Z. Zitouni, A. Bouafia, University of Blida 1, Algeria

A. Limam, University of Lyon, INSA Lyon, MATEIS, CNRS, UMR 5510, 69621 Villeurbanne Cedex, France

are still in progress; even if some questions are solved, some others remain, and the complete seismic design of an earth dam is still an open question.

Stability and safety of earthen dams during an earthquake event are of primary concern. The study of the earth dam's stability under seismic conditions is a challenging problem for geotechnical engineers. In this paper, seismic analysis of an earthen dam is carried out using analytical methods (DYNANSTA software developed here and GEOSTAB software) and software based on finite element method (PLAXIS and ABAQUS).

2 Literature review

Fellenius (1936) developed an ordinary method of slices where the slip area is a circular arc. This method has been extended by other studies under static and pseudo-static conditions (Bishop, 1955; Morgenstern and Price, 1965; Janbu, 1973; Sarma, 1973; Spencer, 1973). In these methods, either force or moment or both force and moment equilibrium of soil mass over failure surface is considered. Soil over it is assumed to be rigid. Kramer (2004) used the limit equilibrium method to evaluate slope stability by supposing that soil at failure follows the perfect plastic Mohr–Coulomb condition. The more commonly used slope stability analyses are based on the limit equilibrium principle (Kahatadeniya et al., 2009; Mendoza et al., 2009; Di Maio et al., 2010; Ferrari et al., 2011; Zheng, 2012).

With regard to the studies conducted through representative tests, Sultan and Seed (1967) have shown, after significant testing on a scaled model, that rupture of the embankment with an inclined core occurs as a result of the movement of two soil blocks (ABCD) (Fig. 1), separated by a thin area, where important shear stress

takes place. More recently, Karbor-e shyadeh and Soroush (2008), Sivakumar Babu et al. (2007) and Özkan et al. (2006) have conducted studies on full-scale real cases and have found that the abrupt rupture of the zoned dams is that of the upstream side.

On the basis of the results of the full-scale tests performed on a shaking table, a recent interesting contribution of Sawada et al. (2018) discusses the seismic performance of small earth dams, with reservoirs on their upstream side repaired with a sloping core zone and geosynthetic clay liners (GCL). Their tests allowed to explain the differences in mechanical behaviour between the upstream and downstream sides of the dam. The results showed that the effective stress of the upstream embankment materials increased because of the undrained shear behaviour of the compacted soils, although deformation on the upstream side was larger than that on the downstream side. Therefore, their tests and analysis led to the conclusion that significant differences occurred in the dynamic behaviour of the upstream side and the downstream side.

In our opinion too, the pore water of the upstream earth dam constituting granular soil cannot drain during an earthquake because of the quake short duration. Then, in this part of the dam, the soil behaviour must be considered as undrained, and the excess pore pressure ΔU developed by a rapid applied loading cannot dissipate instantaneously. The undrained soil mechanical characteristics must be taken into account to study the behaviour under a seismic loading.

Calculation can be addressed generally by two ways, that is, by considering the total stress or the effective stress, where the pore pressure is counted separately. The difficulty resides in the fact that the precise determination of the increase in the actual seismic pore pressure ΔU is

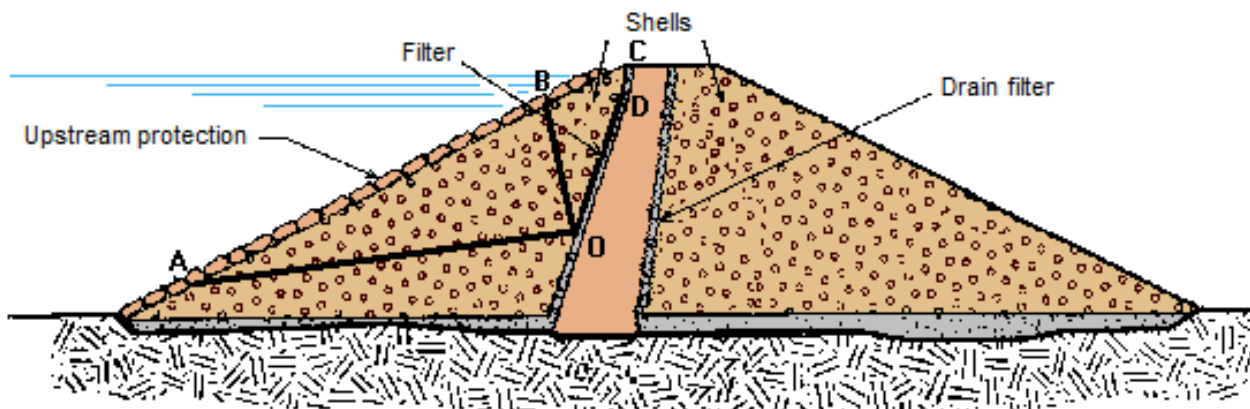


Figure 1: Earth dam.

not an easy task. It is important to underline that this increase or overpressure ΔU can lead to instability of the dam upstream face. Several authors have focused their research efforts on the assessment of ΔU . Some of them are Sarma (1975–1988) and Biondi et al. (2002), and most recently, Tomislav (2006) and Ueng et al. (2010). In the present contribution, the methodology adopted by Sarma was used for the evaluation of the excess pore pressure induced by seismic loading. Between 1975 and 1988, Sarma modified his solution to the problem of stability, which was developed previously in 1973 and was based only on the effective stress analysis. A two-step approach was proposed for determination of the earthquake-induced overpressure.

During the first step, stability has been treated under static loading to derive the total static stresses along the sliding surface. In the second step, stability has been analysed under seismic loading, which allows the calculation of the total dynamic stresses along the considered sliding surface. The difference between the dynamic and the static stresses allows the evaluation of an overload stress $\Delta\sigma$ due to seismic loading. By inserting this value into the Skempton relation (1954), Sarma evaluated the pore pressure ΔU generated by the seismic effect on a granular soil.

This research work focuses on studying the seismic stability of an earth dam based on the following aspects:

1. First, we consider that the slide mechanism of the dam upstream shell occurs by block according to the analysis developed by Sultan and Seed.
2. In the calculation, we consider the undrained characteristics of the granular soil constituting the upstream shell based on the fact that this later cannot drain during a short earthquake.
3. Analysis of the pore pressure generated by an earthquake according to the method developed by Sarma.

Based on these hypotheses and on the limit equilibrium theory, an analytical approach has been developed to study the pseudo-static or seismic stability of an earthen dam constituted of two refills. The upstream and downstream zones are composed of sandy materials, and the waterproof, inclined central core is composed of clayey materials.

Once the pore pressure ΔU due to seismic loading is evaluated, the determination of the seismic pseudo-static safety factor, F_d , which is a function, among others, of this excess pore pressure ΔU can be done. In our analytical study, all the step calculations are considered in a computer program DYNANSTA that was developed by

us. This allows to deduce the effects of several parameters related to the soil characteristics, and to the dam geometry, on its seismic behaviour. In order to identify the influence of each parameter on the seismic behaviour, a parametric study has been conducted and the main results are discussed subsequently and compared to simulations conducted on three well-known software used in geotechnics: GEOSTAB, PLAXIS and ABAQUS.

3 Adaptation of the Sarma calculation to the block method

Effective stress analysis is generally a valid method to analyse any stability problem. Its application in practice is limited to the case where the water pressures are measured or can be estimated with reasonable accuracy, such as for the long-term stability. In general, short-term stability problems require an undrained loading and can be studied using an analysis either by effective stresses with the pore water pressure taken separately or by total stresses. In the effective stress analysis, the water pressure is predicted under real-life testing. However, total stress analysis uses a water pressure value in relation to that at rupture under the undrained test.

The traditional argument when using the effective stress analysis for short-term stability problems is that determination of the deformation depends on these stresses. Therefore, this analysis experiences an insightful perspicacity due to the fact that it requires the determination of actual or exact pressures at the rupture and this is not an easy task.

The analytical approach is based on the following main axes:

1. In the static case, determine the effective principal stresses on each block facet by applying the formula established by Sarma method. Deduce the total principal stresses exercised on each facet by adding the static pore water pressures:

$$\begin{aligned}\sigma_1, o &= \sigma_o + \tau_o (tg\varphi_o + 1/\cos\varphi_o) \\ \sigma_3, o &= \sigma_o + \tau_o (tg\varphi_o - 1/\cos\varphi_o)\end{aligned}$$

2. Since it is impossible, as explained above, to assess directly the effective stresses in the pseudo-static case, the total stresses are evaluated by adding at equilibrium the seismic action to the applied loads. By the same method as in the static case, the total principal stresses are determined as:

$$\sigma_1, d = \sigma_d + \tau_d (tg\varphi_d + 1/\cos\varphi_d)$$

$$\sigma_3, d = \sigma_d + \tau_d (tg\varphi_d - 1/\cos\varphi_d)$$

3. Now that the pseudo-static and static total principal stresses are known, the stress variations on each block rupture facet can be deduced. It will finally allow the evaluation on each block facet of the excess pore pressures due to the earthquake by using the Skempton formula, where A and B are the pore pressure parameters:

$$\Delta U = B [\Delta\sigma_3 + A (\Delta\sigma_1 - \Delta\sigma_3)]$$

4. Considering the pseudo-static state, check the equilibrium of the loads applied to the sliding blocks. The safety factor is a function, among others, of the excess pore pressures generated during the earthquake.

4 Parametric study

4.1 Parameters studied

Table 1 summarises the various parameters proposed in order to analyse their influence on dam stability.

Concerning the variation in parameters, the chosen values are representative of engineer design practice in the field of rammed earth dam. For the justifications of the materials' variation in parameters, we refer to the reports of Kezdi (1974) and Prat et al. (1995). For the sand unit weight, the adopted values are in accordance with the values underlined in the literature. For the other variations in parameters, the proposed values are in the range of the classical variations observed in engineering practice and then allow a correct assessment of the evaluation of the safety factor in the range of the variations considered. Concerning the geometrical parameters of the earth dams, we are interested by the more common configurations. For these cases, the height $H = 50$ m seems to be an upper limit, but exceptions can be much higher. A variation of the angles of upstream and the core are also considered to gauge their effect on stability. The friction angle of a uniform sand is in the range 20° – 30° . The cohesion of saturated clay varies from a few dozen to a few hundred kPa. In our study, the variation was limited to 70 kPa, as our results showed that near this value, the safety factor remains almost constant.

Table 1: Values of different parameters of the problem.

| Parameters | References values | Variations in studied values |
|-----------------------------------------------|----------------------|------------------------------|
| Upstream friction angle (φ) | 25° | 25, 26, 27, 28, 29, 30 |
| Core cohesion (C_u) | 30 kPa | 5, 10, 20, 30, 50, 70 |
| Upstream unit weight (γ) | 20 kN/m ³ | 17, 18, 19, 20, 21, 22 |
| Dam height (H) | 10 m | 10, 15, 20, 30, 40, 50 |
| Slope angle (β) | 21° | 21, 30, 40, 60, 70, 75 |
| Upstream sloping core (α_1) | 31.5° | 31.5, 40, 45, 60, 70, 80 |
| Water level height is taken in the worst case | 8 m | |
| Seismic coefficient spreads in the range | | [0, 0.3] |

4.2 Dam's modelling

In order to gauge the proposed analytical solution, a numerical study of dam's stability subjected to earthquake has been conducted with the pseudo-static method using the following programs:

- GEOSTAB: Based on the limit equilibrium principle, it treats the case of saturated soils by adopting the Bishop method.
- PLAXIS: Based on the finite element method, it is used when considering saturated soil.
- ABAQUS: Based on the finite element method. For these calculations the effect of water was neglected. The results found are interesting, compared to those found by DYNANSTA, where the water effect has been taken into consideration.

The advantages of finite element method have been evaluated for various static slope stability cases (Chang and Huang, 2005), but few comparative studies have been conducted for the computation of the critical seismic coefficient k_c by numerical methods. A major limitation of this method is that it does not provide direct information concerning the safety factor and its corresponding sliding area, which represents an important question for the design and analysis of embankments. Consequently, for this purpose, in this contribution, two techniques have been used which allow calculation of the safety factor by

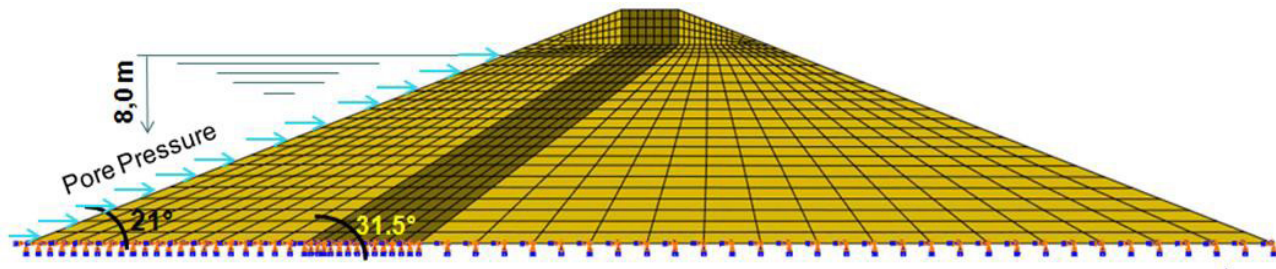


Figure 2: Model geometry and finite element mesh of the embankment with sloping core zone.

the finite element method. The first is the shear strength reduction technique (Zeinkiewicz et al., 1975; Griffiths and Lane, 1999), used by PLAXIS, which consists of reducing the soil shear strength parameters until failure. The second is the gravity-induced method (Swan and Seo, 1999), used in ABAQUS, which consists of increasing the gravitational acceleration until failure. In this study, a two-dimensional finite element model was considered. The meshing was developed using four-node bilinear quadrilateral elements under plane strain condition. The bottom boundary of the model, which coincides with the firm substratum, was clamped (Fig. 2). The mesh density was checked through convergence analysis. The pseudo-static analysis is performed following the three steps given below:

1. Establish the geostatic equilibrium of the dam under its own weight by applying a vertical gravitational acceleration, which permits to calculate the initial stresses due to the weight.
2. Apply gradually a horizontal body force load until failure, where the influence of the earthquake is represented by horizontal seismic coefficient k_h , and apply an additional horizontal motor force $K_h W$ at the centre of gravity of the potential sliding earth volume, with W being its weight.
3. Calculate the safety factor $F = \tau_{\max} / \tau$ for each load increment, and find the seismic acceleration that gives a safety factor equals to 1 (Swan and Seo 1999). The seismic acceleration $a_c = k_c xg$, is considered as the minimum critical acceleration inducing unstable slope. It corresponds to the value 1 of the safety factor.

To simulate the behaviour of the two dams' constitutive soils, clay for the dam core and sandy soil for the shell upstream, an elastoplastic constitutive model was considered. The Mohr–Coulomb failure criteria, characterised by five parameters, was adopted: the elastic modulus E , the Poisson's ratio ν , the friction angle ϕ , the cohesion C_N and the dilatation angle ψ . For a medium sand, which is the most useful configuration, the elastic modulus is in the range 30–50 MPa and for clay with low to

medium plasticity, which is stiff to very stiff, the modulus is in the range 8–30 MPa. These elastic modulus values can be considered as typical according to the guidelines of the Unified Soil Classification (USC) system or according to the typical values of Young's modulus given for granular and cohesive materials by Obrzud and Truty (2012) (see also Kezdi, 1974; Prat et al., 1995). In this studied case, the following values were taken into account: $E = 40$ MPa, $\nu = 0.3$, $\psi = 0^\circ$ for the sand shell upstream and $E = 20$ MPa, $\nu = 0.35$, $\psi = 0^\circ$ for clay constituting the dam core. Previous studies (Griffiths and Lane, 1999; Loukidis et al., 2003) have shown that the elastic modulus and the Poisson's ratio have a negligible effect on the seismic failure. Also, the dilatancy has a negligible effect on the slope's stability (Zeinkiewicz et al., 1975; Griffiths and Lane, 1999).

5 Results and discussion

5.1 Effect of the internal friction angle ϕ

Fig. 3 shows the variation of pseudo-static safety factor F_d versus seismic coefficient k for different soil friction values of ϕ . It is noted that below 27° , the friction angle variation has no significant effect on the safety factor. However, beyond this value, an important increase between 27° and 28° is observed; then, a constant variation of F_d is recorded between 28° and 30° . When the friction angle increases, the dynamic safety factor also increases. It seems that the effect of the friction angle ϕ on the dynamic safety factor F_d is tied to the sand density state. However, the experimental results on sand, obtained by Zitouni (1988) with truly triaxial apparatus, indicate that the friction angle of dense sand is 7° higher than that of loose sand. Based on this result, it can be noted that for low friction angle values, corresponding to the loose state of sand, the increase in pore water pressure ΔU is important. This increase is due to the high void volume between sand grains which conducts to a relatively important quantity

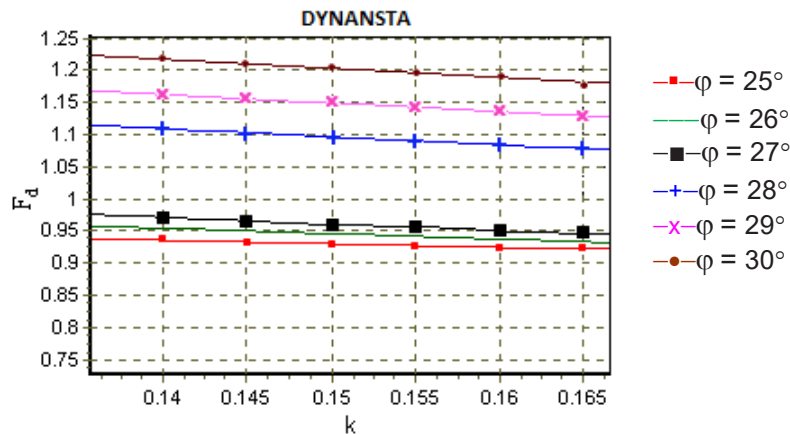


Figure 3: Effect of the internal friction angle.

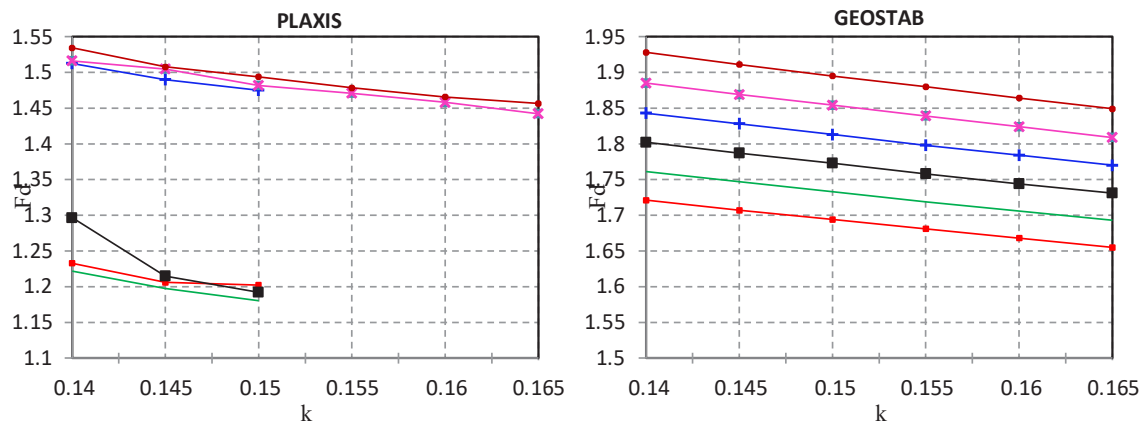


Figure 4: Effect of the internal friction angle with PLAXIS and GEOSTAB.

of absorbed water, indicating a large value of ΔU which is responsible of the safety factor diminution. On the contrary, the important values of ϕ , especially when it exceeds 27° , correspond to the sand state presenting a reduced void volume and containing a low quantity of water, thus generating a limited increase in pore water pressure ΔU with no effect on the safety factor. It is observed in Fig. 4 that with the horizontal seismic coefficient 0.15, the variation of ϕ value between 27° and 30° increases the F_d factor by about 30%, 12% and 27%, respectively, for PLAXIS, GEOSTAB and this study.

5.2 Effect of the seismic coefficient k

The curves shown in Figs 5 and 6 present a practically linear variation between the safety factor F_d and the horizontal seismic coefficient k . The variation of safety factor versus seismic coefficient has been studied by several authors,

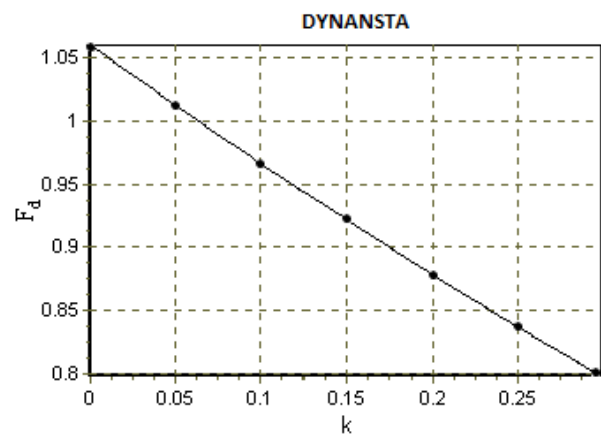


Figure 5: Effect of the seismic coefficient.

and many of them have found an approximately linear relationship between these two parameters.

A significant decrease in the safety factor is noted when the seismic coefficient increases. The stronger

the earthquake is, the weaker the shear strength of soil constituting the dam becomes. Also, when the pore water pressure increases, the structure's safety decreases. The results show that any increase in pseudo-static seismic

coefficient can be considered as a sign of increased horizontal seismic forces, which reduce the safety factor and threatens the dam stability.

Also, the two-dimensional and three-dimensional analyses are in a close agreement with each other in the stability analysis of symmetrical homogeneous slopes (Ahangar-Asr et al., 2012).

5.3 Effect of the core cohesion C_N

Fig. 7 shows that when the core cohesion increases, the safety factor also increases, but with a lesser amplitude when the seismic coefficient increases. For the seismic coefficient $k = 0.05$ and soil cohesion $C_N = 50$ kPa, F_d is more or less 5% higher than the case corresponding to the soil cohesion $C_N = 5$ kPa. In contrast, for a seismic coefficient $k = 0.3$, the difference between the safety factors F_d is only around 3%, for the same soil cohesion values discussed before. This discrepancy suggests that for a high value of k , corresponding to higher seismic load, the pore water pressure value ΔU becomes higher, implying a reduction in the safety factor F_d . Furthermore, the other result shown by this illustration is that for cohesion values greater than or equal to 70 kPa, the safety factor varies with the increase in the seismic coefficient k , with a value always exceeding 1. It seems that beyond the value of 70 kPa, the increasing ΔU has an insignificant effect on the safety factor. This can be explained by the fact that the soil cohesion in these cases corresponds to a high number of contacts, and thus to a less important void between soil particles. Then, the small quantity of water cannot develop an important value of ΔU . It is noted in Fig. 8 that the difference between F_d given by PLAXIS and this study is around 17.98% for $k = 0.15$ and for $C_N = 70$ kPa.

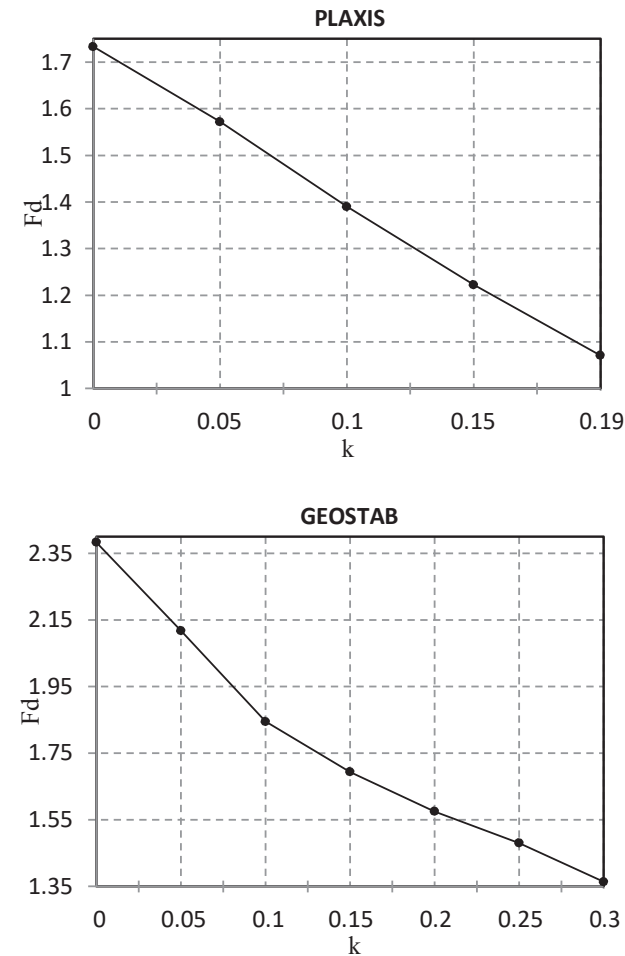


Figure 6: Effect of the seismic coefficient with PLAXIS and GEOSTAB.

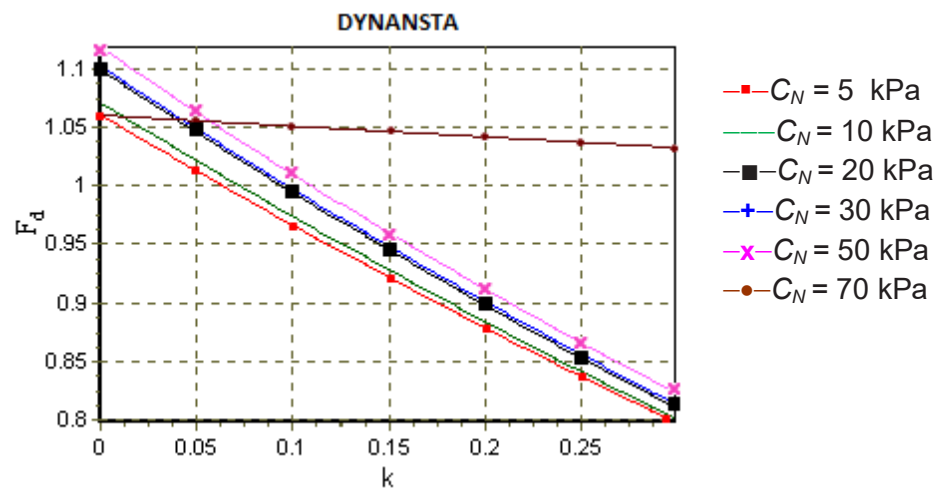


Figure 7: Effect of the core cohesion.

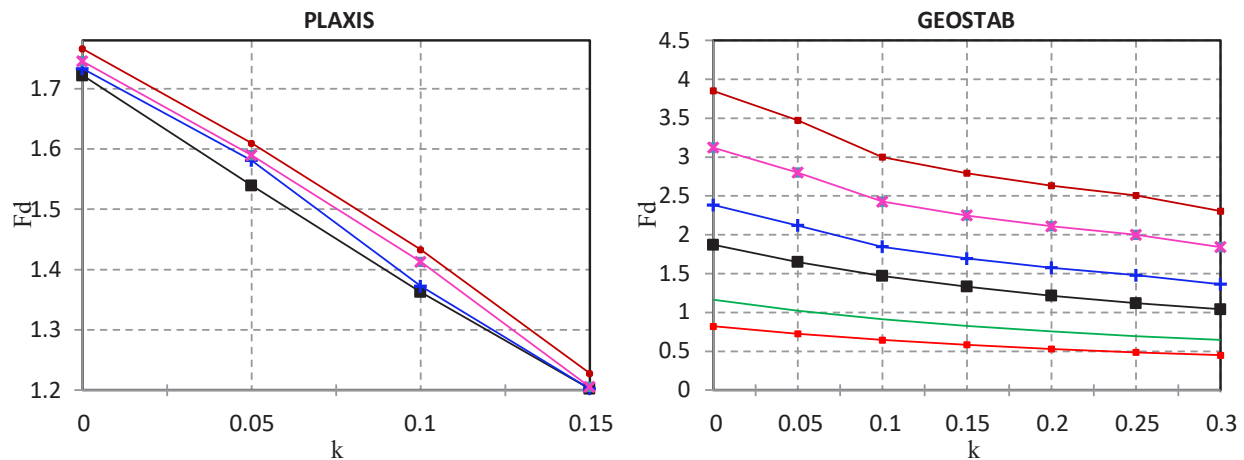


Figure 8: Effect of the core cohesion with PLAXIS and GEOSTAB.

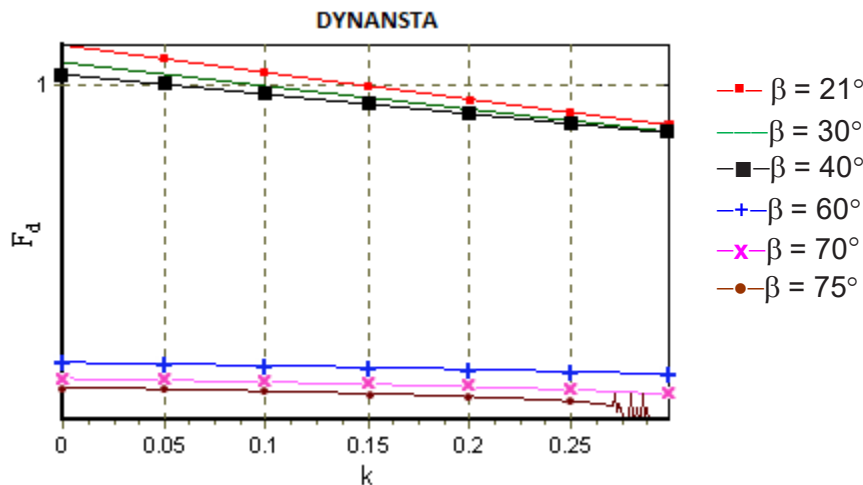


Figure 9: Effect of the slope angle.

In addition, the effect of excess pore pressure generated by the earthquake is neglected in the GEOSTAB study, which gives higher safety factors.

5.4 Effect of the slope angle β

The curves in Figs 9 and 10 show that the slope has a dominant role in the structure's stability. The safety factor decreases gradually when the inclination of the slope increases. For $k = 0.15$ and $\beta = 21^\circ$, the difference between the safety factor given by the two software programs and our calculation is around 20% compared to PLAXIS and 69.4% compared to GEOSTAB. It is also noted that for a seismic coefficient equal to 0.3, when the slope angle increases from 21° to 70° , the stability is reduced by 75%

in this study and by 31% in the analysis conducted by the Bishop method. This reduction (see Fig. 9) is about 83%, 90% and 100% for the coefficients 0.2, 0.1 and under static conditions, respectively. Therefore, the failure mechanism is really important in this studied case. It is necessary to know which part of the structure would be seriously distorted and where the critical slip area could be. This analysis allowed to have noticeable conclusions on the mechanism, the position and the non-circular slip form for this type of dam.

5.5 Effect of the upstream sloping core α_1

It is noticeable from the slope variation curves of the upstream core in Figs 11 and 12 that the safety factor

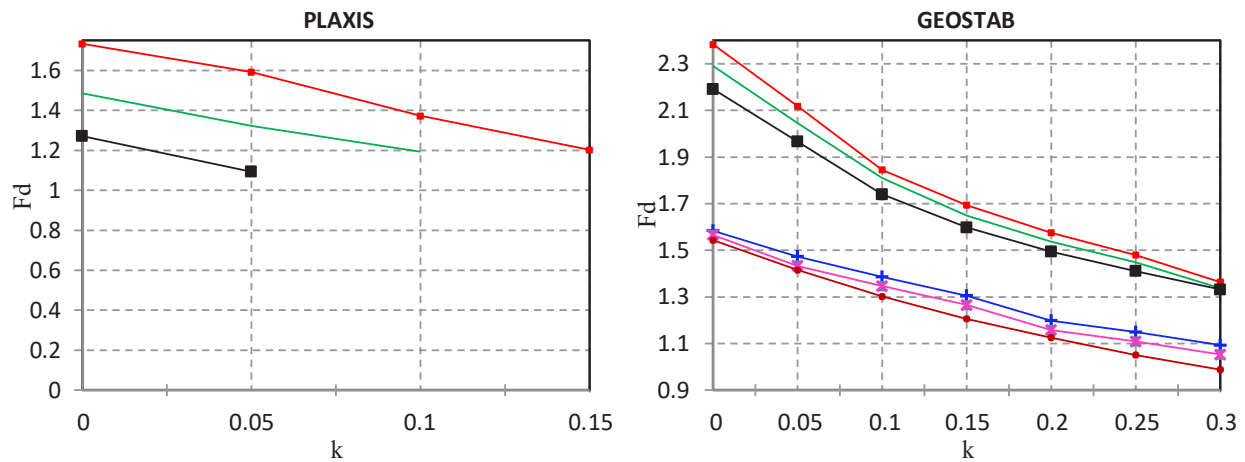


Figure 10: Effect of the slope angle with PLAXIS and GEOSTAB.

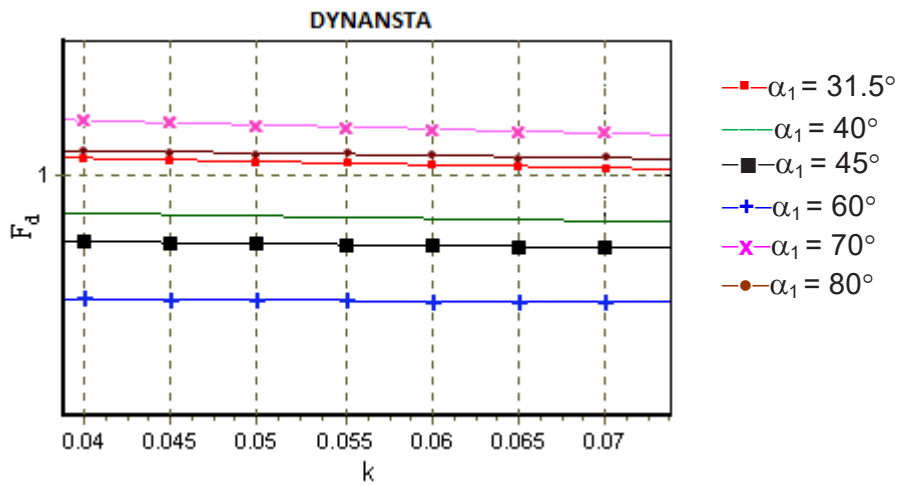


Figure 11: Effect of the upstream sloping core.

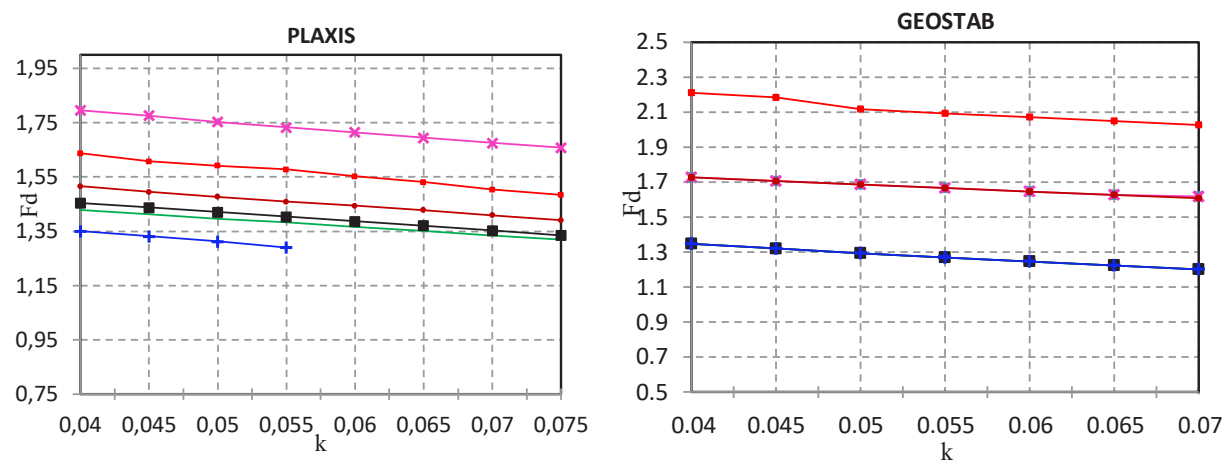


Figure 12: Effect of the upstream sloping core with PLAXIS and GEOSTAB.

decreases when the sloping core increases. It starts to increase from a certain level where the tilt approaches the vertical. For a 70° slope, with a seismic coefficient equal to 0.07, the results show a difference of around 31.8% compared to GEOSTAB and around 37.58% compared to PLAXIS. It is noticed that the values of the safety factor, corresponding to a slope higher than 31.5° and lower than 70° , remain constant (along the seismic coefficient interval studied) and are less than 1. For these particular physical and mechanical soil characteristics and geometrical data of the earth dam, it seems that the slope of 70° presents an improved solution. Therefore, it can be noted that the increase in the core slope ensures a higher resistance to the seismic slip of structures whose height is less than 15 m.

5.6 Effect of dam's height H

It is noted that for the same upstream shell material and the same core material characterised by the physical and mechanical characteristics described above, the height has a negative impact on the safety against sliding. For heights greater than 20 m, the variation curves of heights in Fig. 13 keep the same form, and the safety factor is at all times less than 1, regardless the seismic coefficient k . It is also noted in Fig. 14 that for a 15 m height, and with $k = 0.1$, the difference in F_d between PLAXIS and the proposed solution is around 9%. Concerning the case of the 15-m-height dam, the pseudo-static safety factor is less compared to the 10-m-height dam, when $k > 0.12$. This underlines that for a given set of physical and mechanical soil parameters, the related set of the dam geometric parameters needs to be respected and taken into account.

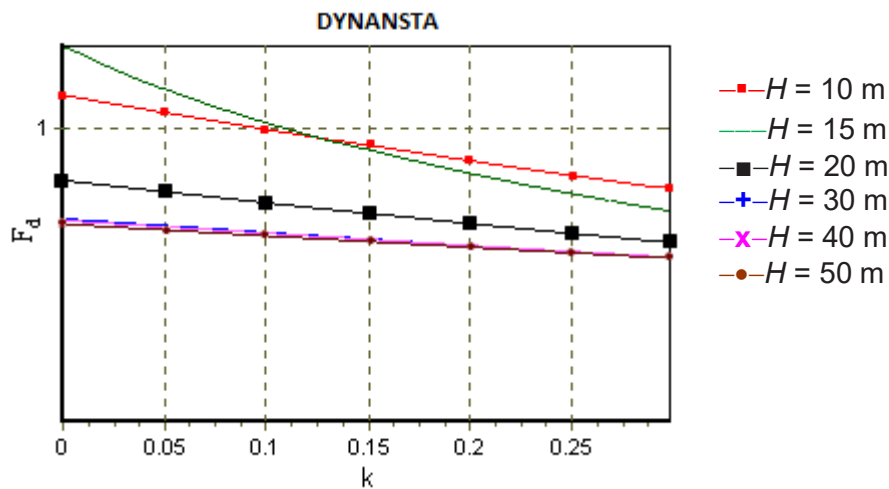


Figure 13: Effect of dam's height.

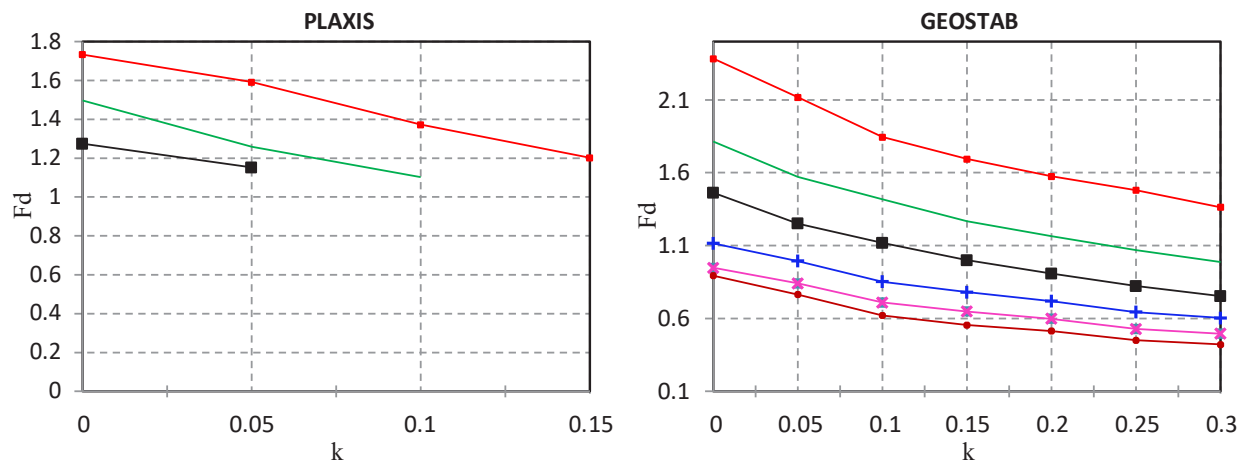


Figure 14: Effect of dam's height with PLAXIS and GEOSTAB.

5.7 Effect of the upstream unit's weight γ

The interpretation of the results shown in Fig. 15 suggests that for a given seismic coefficient value, the seismic safety factor is nearly constant when the unit weight value is below 19 kN/m³ or beyond 20 kN/m³. However, between these two values, it is noted that, as for the friction angle effect, there is a substantial increase in the F_d value reaching at least four times. It seems that here too, this increase can be explained that for values less than or equal to 19 kN/m³, the void volume is relatively large, involving the seismic pore pressure ΔU that significantly affects the safety factor and makes it almost null. On the contrary, for unit weight values greater than or equal to 20 kN/m³, the effect of ΔU becomes increasingly significant with the increase of the earthquake amplitude represented by the seismic coefficient k . In other words, when k increases, the F_d decreases rather quickly. It is noted that for the values $k = 0.15$ and $\gamma = 22$ kN/m³, the difference between F_d of this study and the one given by PLAXIS in Fig. 16 is around 24%. This leads to conclude that the rupture

risk of the dam's upstream side is higher than that of the downstream side studied by PLAXIS.

5.8 Stability in the critical state: Comparison of results with those of the other methods

The critical seismic acceleration corresponds to the minimum value, beyond which the upstream face of the dam becomes unstable. It corresponds to the value 1 of the safety factor. Here, the earthquake's horizontal component is mainly considered, since the vertical component has nearly no effect on the dam instability. Based on the results given in Table 2, the critical seismic coefficient K_c assessed by the present method is smaller than that of all the other methods considered here. The risk of instability in this case is, therefore, more important. It can also be noted that when the clay core cohesion varies between 10 and 70 kPa, the maximum difference Δ_{\max} between the seismic value K_c of the proposed method and that of others is about 8% for PLAXIS, 28% for ABAQUS and 46%

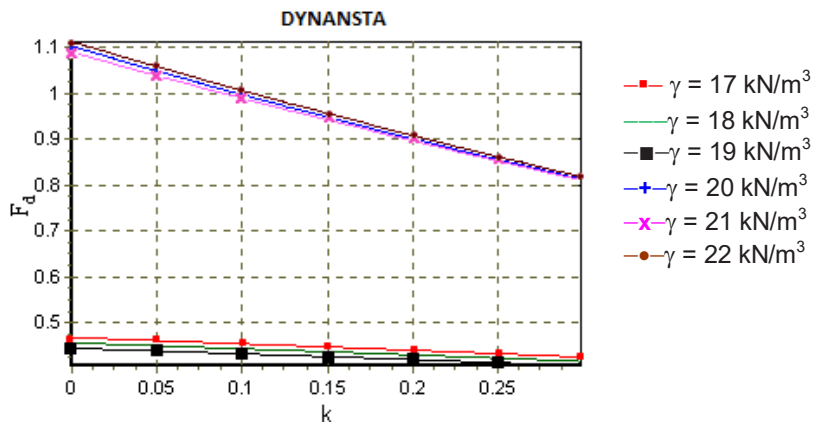


Figure 15: Effect of the upstream unit's weight.

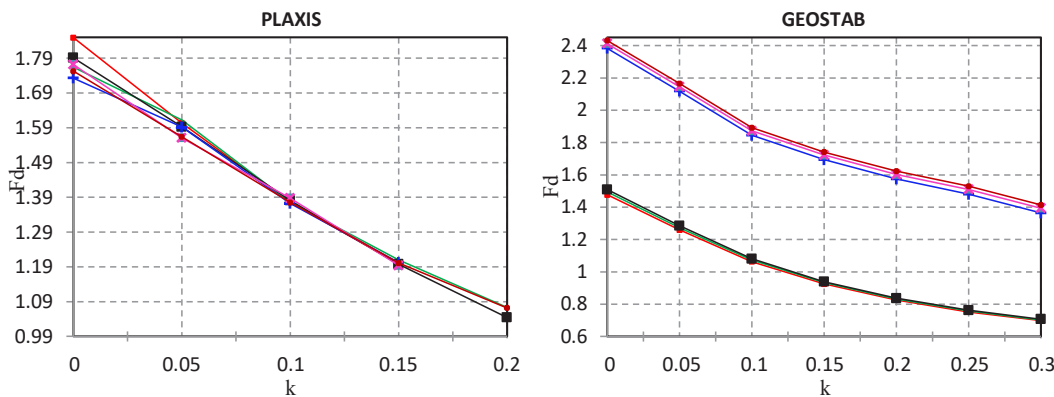
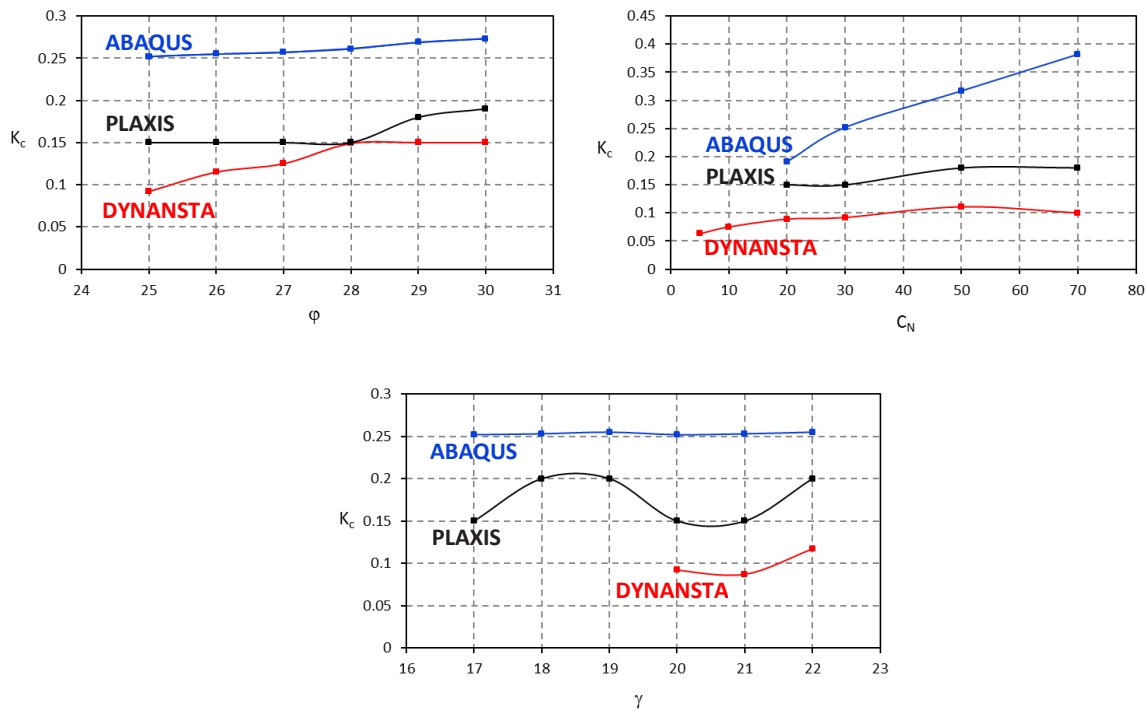


Figure 16: Effect of the upstream unit's weight with PLAXIS and GEOSTAB.

Table 2: Comparison of K_c at critical state of the different methods.

| $\varphi(^{\circ})$ | γ (kN/m ³) | DYNANSTA | | | PLAXIS | | | ABAQUS | | | GEOSTAB | | |
|---------------------|-------------------------------|-------------|----------|-------|--------|-------|----------|--------|-------|----------|---------|-------|----------|
| | | C_N (kPa) | K_c | F_d | K_c | F_d | Δ | K_c | F_d | Δ | K_c | F_d | Δ |
| | 5 | | 0.063 | 1 | - | - | - | - | - | - | - | < 1 | - |
| | 10 | | 0.075 | 1 | - | - | - | - | - | - | 0.05 | 1.024 | -2.5 |
| | 20 | | 0.089 | 1 | 0.15 | 1.202 | 6.08 | 0.191 | 1.139 | 10.18 | 0.3 | 1.042 | 21.08 |
| | 30 | | 0.092 | 1 | 0.15 | 1.202 | 5.80 | 0.252 | 1.165 | 16 | 0.401 | 1.12 | 30.90 |
| | 50 | | 0.111 | 1 | 0.18 | 1.094 | 6.94 | 0.317 | 1.247 | 20.64 | 0.55 | 1.051 | 43.94 |
| | 70 | | 0.1 | 1.05 | 0.18 | 1.141 | 8 | 0.382 | 1.31 | 28.2 | 0.558 | 1.056 | 45.8 |
| 25 | | | 0.092 | 1 | 0.15 | 1.202 | 5.80 | 0.252 | 1.165 | 16 | 0.401 | 1.12 | 30.90 |
| 26 | | | 0.115 | 0.953 | 0.15 | 1.181 | 3.5 | 0.255 | 1.169 | 14 | 0.45 | 1.039 | 33.5 |
| 27 | | | 0.125 | 0.938 | 0.15 | 1.192 | 2.5 | 0.257 | 1.173 | 13.2 | 0.521 | 1.014 | 39.6 |
| 28 | | | 0.149 | 1.1 | 0.15 | 1.475 | 0.1 | 0.261 | 1.179 | 11.2 | 0.532 | 0.972 | 38.3 |
| 29 | | | 0.15 | 1.15 | 0.18 | 1.108 | 3.01 | 0.269 | 1.183 | 11.9 | 0.5 | 0.994 | 35 |
| 30 | | | 0.15 | 1.2 | 0.19 | 1.071 | 4 | 0.273 | 1.188 | 12.3 | 0.5 | 1.025 | 35 |
| | 17 | | [0, 0.3] | < 1 | 0.15 | 1.198 | - | - | - | - | 0.1 | 1.063 | - |
| | 18 | | [0, 0.3] | < 1 | 0.2 | 1.073 | - | - | - | - | 0.108 | 1.07 | - |
| | 19 | | [0, 0.3] | < 1 | 0.2 | 1.044 | - | - | - | - | 0.121 | 1.009 | - |
| | 20 | | 0.092 | 1 | 0.15 | 1.202 | 5.80 | 0.252 | 1.165 | 16 | 0.401 | 1.12 | 30.90 |
| | 21 | | 0.087 | 1 | 0.15 | 1.194 | 6.28 | 0.253 | 1.182 | 16.58 | 0.445 | 1.109 | 35.78 |
| | 22 | | 0.117 | 1 | 0.2 | 1.072 | 8.35 | 0.255 | 1.19 | 13.85 | 0.473 | 1.11 | 35.65 |

**Figure 17:** K_c critical state values according to the different variations.

for GEOSTAB. Similarly, for a variation of the friction angle between 25° and 30° , the difference Δ_{\max} is about 5.8% for PLAXIS, 16% for ABAQUS and 39.6% for GEOSTAB. It is also seen that this difference is about 8.35% for PLAXIS, 16.58% for ABAQUS and 35.78% for GEOSTAB when the sand soil unit weight, constituting the upstream shell, varies between 17 and 22 kN/m³.

The following can be concluded from these results:

- The presence of central core tilted to the downstream has permitted a good clamping of the core, which provides a better resistance against the reservoir water pressure. Therefore, ΔU generated on the upstream slope has caused a limit state more critical and faster in time.
- The extent of the sliding movement of the upstream slope in this study is more abrupt and occurs before that of the downstream slope analysed by PLAXIS. So, the instability conditions of the upstream slope are more critical than those of the downstream slope.
- Generally, the block method and the shear strength reduction technique give F_d and K_c lower than those given by the gravity increase and Bishop's modified methods. This difference can be attributed to the effects of ΔU pressures neglected in these last two methods.

The numerous treated cases lead to conclude that the dam embankment pore overpressure ΔU , caused by the characteristic cyclic loadings of an earthquake, affects its structural stability drastically. The cases studied here suggest that the structure of a zoned earth dam requires more specific analysis.

The results, compared to those obtained on various structures such as earth dams, retaining walls, breakwaters wall (Yu et al., 2005; Choudhury and Mohd. Ahmed, 2007; Colomer Mendoza et al., 2009; Moayedi et al., 2010; Cihan et al., 2012), give the same profiles of the safety factor variation related to the various parameters considered.

The curves found in Fig. 17 show that the critical seismic coefficient K_c , evaluated by our method, is smaller than the one obtained by the other methods. Thus, our proposed method is more conservative. Higher K_c coefficients are systematically obtained with ABAQUS code. This is explained by the fact that the effect of water is neglected here.

6 Conclusions

To gauge the behaviour of a sloping core earth dam undergoing a seismic loading, an analytical calculation method was developed that allows the evaluation of the safety factor relative to the stability in sliding of the upstream slope. This safety factor especially considers the pore water overpressure ΔU that develops in the cohesionless soil constituting the upstream recharge. Indeed, during an earthquake, water develops an excess of pore pressure ΔU , and this overpressure cannot dissipate during the very short seismic shaking duration.

To evaluate the safety factor, a set of parameters has been considered, both those related to soil (cohesion C_u , friction angle ϕ , unit weight γ) and those related to the geometry of the dam (upstream slope, dam height, upstream sloping core). Based on the established comparative study, it is concluded that the sliding movement extent of the upstream slope is more abrupt and occurs before that of the downstream slope analysed by PLAXIS. So, the upstream slope is in a most critical condition than the downstream slope. It was also noticed that the block method gives F_d and K_c lower than those given by the gravity increase and Bishop's modified methods. It seems that this difference can be due to the effects of ΔU overpressures neglected in these last two methods. This analysis allowed us to have clear conclusions about the mechanism, the position and the non-circular slip form for the type of dams considered here.

According to our results, for a given dam section and a set of mechanical and physical parameters of the soil, the progressive increase in pore pressure due to the increase in the interstitial overpressure ΔU induces a loss of shear strength of the soil. This is the major reason for the upstream slope instability.

Through this parametric study, admitting a sliding by blocks, it is noted that, the physical and mechanical soil characteristics, the dam geometrical parameters and the seismic coefficient have a great influence on the safety factor value. In order to ensure the stability of a zoned dam, we suggest to adopt a well-defined set of dam geometric parameters and the actual mechanical and physical soil properties based on accurate soil study. Finally, the design of inclined core dams in seismic zones is mandatory.

References

- [1] ABAQUS V.610 (2010) Manuel.
- [2] Ahangar-Asr, A., Toufigh, M.M., Salajegheh, A., 2012. Determination of the most probable slip surface in 3D slopes considering the effect of earthquake force direction. *Computers & Geosciences*, Volume 45, pp. 119-130.
- [3] Bakir, B.S., Akiş, E., 2005. Analysis of highway embankment failure associated with the 1999 Düzce, Turkey earthquake. *Soil Dynamics and Earthquake Engineering*, Volume 25, pp. 251-260.
- [4] Basudhar, P.K., Rao, N.S.V. K., Bhokya, M., and Dey, A., (2010) "2D FEM Analysis of Earth and Rockfill Dams under Seismic Condition". Fifth International conference on Recent Advances in Geotechnical Earthquake Engineering and Soil Dynamics", San Diego California. May 24-29 2010.
- [5] Biondi, G., Cascone, E., Maugerie, M., Motta, E., 2000. Seismic response of saturated cohesion less slopes. *Soil Dynamics and Earthquake Engineering*, Volume 26, pp. 209-215.
- [6] Biondi, G., Cascone, E., Maugerie, 2002. Flow and deformation failure of sandy slopes. *Soil Dynamics and Earthquake Engineering*, Volume 22, Issues 9-12, pp. 1103-1114.
- [7] Bishop, A.W., 1955. The use of the slip circle in the stability analysis of slopes. *Geotechnique*, Volume 5, Issue 1, March 1955, pp. 7-17.
- [8] Chang, Y. L., Huang, T. K., 2005. Slope stability analysis using strength reduction technique. *Journal of the Chinese Institute of Engineers*, Volume 28 (2), pp. 231-240.
- [9] Choudhury, D., Mohd. Ahmed, S., 2007. Stability of water front retaining wall subjected to pseudo-static earthquake forces. *Ocean Engineering*, Volume 34, pp. 1947-1954.
- [10] Cihan, K., Yuksel, Y., Berilgen, M., Cevik, E.O., 2012. Behavior of homogeneous rubble mound breakwaters materials under cyclic loads. *Soil Dynamics and Earthquake Engineering*, Volume 34, pp. 1-10.
- [11] Colomer Mendoza, F.J., Ferrer Gisbert, A., Gallardo Izquierdo, A., Bovea, M.D., 2009. Safety factor nomograms for homogeneous earth dams less than ten meters high. *Engineering Geology*, Volume 105, pp. 231-238.
- [12] Di Maio, C., Vassallo, R., Vallario, M., Pascale, S., Sdao, F., 2010. Structure and kinematics of a landslide in a complex clayey formation of the Italian Southern Apennines. *Engineering Geology*, Volume 116, Issues 3-4, pp. 311-322.
- [13] Fellenius, W., 1936. Calculation of the stability of earth dams. *Proceedings of 2nd Congress on Large Dams*, Volume 4, pp. 445-463.
- [14] Ferrari, A., Ledesma, A., Gonzalez, D.A., Corominas, J., 2011. Effects of the foot evolution on the behaviour of slow-moving landslides. *Engineering Geology*, Volume 117, pp. 217-228.
- [15] GEOSTAB V4.07 (2013) Manuel.
- [16] Griffiths, D. V., Lane, P. A., 1999. Slope stability analysis by finite elements. *Geotechnique*, Volume 49 (3), pp. 387-403.
- [17] Hori, T., Ueno, K., Matsushima, K., 2012. Damages of small earth dams induced by the 2011 earthquake of the Pacific Coast of Tohoku. Technical Report in NIRE, 213, pp. 175-199 (in Japanese).
- [18] Janbu, N., 1973. Slope stability computations, *Embankment-Dam Engineering*. In: Hirschfeld, R.C., Poulos, S.J. (Eds.), Casagrande Volume. John Wiley & Sons, pp. 47-86.
- [19] Kahatadeniya, K.S., Nanakorn, P., Neaupane, K.M., 2009. Determination of the critical failure surface for slope stability analysis using ant colony optimization. *Engineering Geology*, Volume 108 (1-2), pp. 133-141.
- [20] Karbor-e- shyadeh, A.H., Soroush, A., 2008. A comparison between seismic behaviors of earth dams with inclined and vertical clay cores a numerical analysis approach. The 14th World Conference on Earthquake Engineering, October 12-17, 2008, Beijing, China.
- [21] Kezdi, A. (1974). *Handbook of Soil Mechanics*. Elsevier, Amsterdam.
- [22] Loukidis, D., Bandini, P., Salgado, R., 2003. Stability of seismically loaded slopes using limit analysis. *Geotechnique*, Volume 53 (5), pp. 463-479.
- [23] Maula, B.H., Zhang, L., 2011. Assessment of embankment factor safety using two commercially available programs in slope stability analysis. *Procedia Engineering*, Volume 14, pp. 559-566.
- [24] Mendoza, F.J.C., Gisbert, A.F., Izquierdo, A.G., Bovea, M.D., 2009. Safety factor nomograms for homogeneous earth dams less than ten meters high. *Engineering Geology*, Volume 105, pp. 231-238.
- [25] Moayedi, H., B.K. Huat, B., Mohamed Ali, T.A., Haghighi, A.T., Asadi, A., 2010. Analysis of longitudinal cracks in crest of Doroodzan dam. *EJGE* 15, Bund. D, pp. 337-347.
- [26] Mohri, Y., Masukawa, S., Hori, T., Ariyoshi, M., 2014. Damage to agricultural facilities. *Soils Found.* 54 (4), 588-607.
- [27] Morgenstern, N.R., Price, V.E., 1965. The analysis of the stability of general slip surfaces. *Geotechnique*, Volume 15, pp. 9-93.
- [28] Obrzud, R., Truty, A. The Hardening Soil Model: A Practical Guidebook in Zsoil. PC 100701 report, revised 31.01.2012.
- [29] Özkan, M.Y., Özyazicioglu, M., Aksar, U.D., 2006. An evaluation of Güldürcek dam response during 6 June 2000 Orta earthquake. *Soil Dynamics and Earthquake Engineering*, Volume 26, pp. 405-419.
- [30] PLAXIS V8.2 Manuel.
- [31] Prat, M., Bisch, E., Millard, A., Mestat, P., and Cabot, G. (1995). *La modélisation des ouvrages*. Hermes, Paris.
- [32] Sarma, S.K., 1973. Stability analysis of embankments and slopes. *Geotechnique*, Volume 23 (3), pp. 423-433.
- [33] Sarma, S.K., 1975. Seismic stability of earth dams and embankments. *Geotechnique*, Volume 25 (4), pp. 743-761.
- [34] Sarma, S.K., 1979. Response and stability of earth dams during strong earthquakes. Report Misc. GL-79-13, US Corps of Engineers, Vicksburg, Miss., USA.
- [35] Sarma, S.K., 1981. Seismic displacement analysis of earth dams. *Journal Geotechnical Engineering Division, ASCE*, 107, GT12, pp. 1735-1739.
- [36] Sarma, S.K., 1988. Seismic response and stability of earth dams. *Seismic risk assessment and design of building structures*, Ed. A. Koridze, Omega Scientific, pp. 143-160.
- [37] Sarma, S.K., Barbosa, M.R., 1985. Seismic stability analysis for rockfill with central clay cores. *Geotechnique*, Volume 35(3), pp. 319- 328.
- [38] Sarma, S.K., Chowdhury, R.N., 1996. Simulation of pore pressures in earth structures during earthquakes. Eleventh World Conference on Earthquake Engineering.
- [39] Sarma, S.K., Jennings, D.N., 1980. A dynamic pore pressure parameter An. Proc. Int. Symp. Soils Under Cyclic and

- Transient Loading, Ed. Pande, Swansea, England, 1 (2), pp. 295-298.
- [40] Sawada, Y., Nakazawa, H., Oda, T., Kobayashi, S., Shibuya, S., Kawabata, T., 2018. Seismic performance of small earth dams with sloping core zones and geosynthetic clay liners using full-scale shaking table tests. *Soils and Foundations* 58 (2018) 519–533.
 - [41] Seed, H.B., Lee, K.L., Idriss, I.M., Makdisi, F., 1973. Analysis of the slides in the San Fernando Dams during the earthquake of February 9 1971. Report No. UCB/EERC-88/04, University of California, Berkeley, CA, USA.
 - [42] Seed, H.B., Sultan, H.A., 1967. Stability analysis for a sloping core embankment. *Journal of the Soil Mechanics and Foundation Division. ASCE*, Volume 93 (4), pp. 69-83.
 - [43] Sivakumar Babu, G.L., Amit Srivastava, Sahana, V., 2007. Analysis of stability of earthen dams in kachchh region, Gujarat, India. *Engineering Geology*, Volume 94, Issues 3-4, Pages 123–136.
 - [44] Spencer, E., 1973. Thrust line criterion in embankment stability analysis. *Geotechnique*, Volume 23 (1), pp. 85–100.
 - [45] Sultan, H.A., Seed, H.B., 1967. Stability of sloping core earth dams. *Journal of the Soil Mechanics and Foundation Division. ASCE*, Volume 93 (4), pp. 45-67.
 - [46] Swan, C. C., Seo, Y.-K., 1999. Limit state analysis of earthen slopes using dual continuum/FEM approaches. *International Journal for Numerical and Analytical Methods in Geomechanics*, Volume 23 (12), pp. 1359-1371.
 - [47] Tani, S., 1996. Damage to earth dams. *Soils Found.* 36, 263–272.
 - [48] Tomislav, I., 2006. A model for presentation of seismic pore water pressures. *Soil Dynamics and Earthquake Engineering*, Volume 26, pp. 191-199.
 - [49] Ueng, T.S., Wu, C.W., Cheng, H.W., Chen, C.H., 2010. Settlements of saturated clean sand deposits in shaking table tests. *Soil Dynamics and Earthquake Engineering*, Volume 30, pp. 50-60.
 - [50] Ueng, T.S., Wu, C.W., Lin, C.Y., Yu, R.Y., 2000. Pore water pressure changes in sands under earthquake loading. 12th World Conference on Earthquake Engineering.
 - [51] Yu, Y., Xie, L., Zhang, B., 2005. Stability of earth-rockfill dams: Influence of geometry on the three-dimensional effect. *Computers and Geotechnics*, Volume 32, pp. 326-339.
 - [52] Yuan, L., Liu, X., Wang, X., Yang, Y., Yang, Z., 2014. Seismic performance of earth-core and concrete faced rock-fill dams by large-scale shaking table tests. *Soil Dyn. Earthquake Eng.* 56, 1-12.
 - [53] Zheng, H., 2012. A three-dimensional rigorous method for stability analysis of landslides. *Engineering Geology*, Volume 145–146, pp. 30–40.
 - [54] Zienkiewicz, O. C., Humpheson, C., Lewis, R.W., 1975. Associated and non associated visco-plasticity and Plasticity in soil mechanics. *Geotechnique*, Volume 25 (4), pp. 671-689.
 - [55] Zitouni, Z., 1985 Calcul de stabilité aux séismes des talus de barrages en terre par la méthode des blocs. Mémoire de D.E.A, présentée à l'université scientifique et Médicale de Grenoble.
 - [56] Zitouni, Z., 1988. Comportement tridimensionnel des sables. Thèse de doctorat, université Joseph Fourier, Grenoble I.